

Quartic Gauge Boson Couplings ^{*}

HONG-JIAN HE

*Department of Physics and Astronomy, Michigan State University
 East Lansing, Michigan 48824, USA
 (E-mail: hjhe@pa.msu.edu)*

Abstract. We review the recent progress in studying the anomalous electroweak quartic gauge boson couplings (QGBCs) at the LHC and the next generation high energy $e^\pm e^-$ linear colliders (LCs). The main focus is put onto the strong electroweak symmetry breaking scenario in which the non-decoupling guarantees sizable new physics effects for the QGBCs. After commenting upon the current low energy indirect bounds and summarizing the theoretical patterns of QGBCs predicted by the typical resonance/non-resonance models, we review our systematic model-independent analysis on bounding them via WW -fusion and WWZ/ZZZ -production. The interplay of the two production mechanisms and the important role of the beam-polarization at the LCs are emphasized. The same physics may be similarly and better studied at a multi-TeV muon collider with high luminosity.

PACS number(s): 11.30.Qc, 11.15.Ex, 12.15.Ji, 14.70.Pw

1. Introduction

The non-Abelian gauge structure of the standard model (SM) predicts the presence of electroweak quartic gauge boson couplings (QGBCs) besides the couplings of triple gauge bosons. The electroweak symmetry breaking (EWSB) sector involves the would-be Goldstone boson [1] dynamics which generates the longitudinal components for W^\pm, Z^0 so that they acquire the observed masses. Despite the astonishing success of the SM at scales up to $O(100\text{GeV})$ [2,3], this EWSB sector remains unverified [4]. Any new physics in the underlying Goldstone boson dynamics will cause the gauge boson self-interactions to deviate from the SM. The quartic gauge boson interactions are particularly interesting because they can involve four longitudinal components which, according to the equivalence theorem [5,6], manifest at high energies as pure Goldstone boson interactions (that is independent of the SM gauge couplings). To

^{*}) Invited talk presented at the Workshop on “*Physics at the First Muon Collider and at the Front End of a Muon Collider*”, November 6-9, 1997, at Fermi National Accelerator Laboratory, Batavia, IL, USA. To be published in the conference proceedings, eds. S. Geer and R. Raja.

unambiguously test the couplings of the quartic gauge boson interactions (QGBCs), the high energy WW -fusion and triple gauge boson production processes have to be used, where the QGBCs directly appear at the tree level. It is therefore important to study how the future high energy colliders (such as the CERN LHC and $e^\pm e^-$ linear colliders [7,8]) can sensitively probe the QGBCs for unveiling the mystery of the EWSB mechanism.

The EWSB sector can interact weakly or strongly. The weakly coupled case (such as supersymmetric models [9]) ensures the new physics at higher scales to have *decoupling* property [10] at low scales, while in the strongly interacting scenario [11] the nondecoupling guarantees the new physics scale to lie below or at $4\pi v \sim 3$ TeV [12]. In the former case the light Higgs boson(s) plus superpartners have to be first discovered, while for the latter we expect sizable new physics deviations showing up in the quartic (and triple) gauge boson couplings, which is the focus of this review. Below the new physics scale Λ , all the new physics effects in the EWSB sector can be parametrized by a complete set of the next-to-leading order (NLO) effective operators of the electroweak chiral Lagrangian (EWCL) [13], in which the $SU(2)_L \otimes U(1)_Y$ gauge symmetry is nonlinearly realized¹. Without experimental observation on any new light resonance [2,3], this effective field theory approach [14,12] provides the most economic description of the possible new physics effects. Among the complete set of the fifteen NLO operators, five of them characterize only the quartic gauge interactions [13]:

$$\left\{ \begin{array}{l} \mathcal{L}_4 = \ell_4 \left(\frac{v}{\Lambda}\right)^2 [\text{Tr}(\mathcal{V}_\mu \mathcal{V}_\nu)]^2, \\ \mathcal{L}_5 = \ell_5 \left(\frac{v}{\Lambda}\right)^2 [\text{Tr}(\mathcal{V}_\mu \mathcal{V}^\mu)]^2; \end{array} \right. \quad (\text{SU}(2)_c: \checkmark) \quad (1)$$

$$\left\{ \begin{array}{l} \mathcal{L}_6 = \ell_6 \left(\frac{v}{\Lambda}\right)^2 [\text{Tr}(\mathcal{V}_\mu \mathcal{V}_\nu)] \text{Tr}(\mathcal{T} \mathcal{V}^\mu) \text{Tr}(\mathcal{T} \mathcal{V}^\nu), \\ \mathcal{L}_7 = \ell_7 \left(\frac{v}{\Lambda}\right)^2 [\text{Tr}(\mathcal{V}_\mu \mathcal{V}^\mu)] \text{Tr}(\mathcal{T} \mathcal{V}_\nu) \text{Tr}(\mathcal{T} \mathcal{V}^\nu), \\ \mathcal{L}_{10} = \ell_{10} \left(\frac{v}{\Lambda}\right)^2 \frac{1}{2} [\text{Tr}(\mathcal{T} \mathcal{V}^\mu) \text{Tr}(\mathcal{T} \mathcal{V}^\nu)]^2. \end{array} \right. \quad (\text{SU}(2)_c: \times)$$

In (1), $\mathcal{V}_\mu \equiv (D_\mu U)U^\dagger$, $D_\mu U = \partial_\mu U + \mathbf{W}_\mu U - U \mathbf{B}_\mu$, $\mathbf{W}_\mu \equiv igW_\mu^a \tau^a/2$, $\mathbf{B}_\mu \equiv ig'B_\mu \tau^3/2$, $U = \exp[i\tau^a \pi^a/v]$ (with π^a the would-be Goldstone boson field), and $\mathcal{T} \equiv U \tau_3 U^\dagger$ is the custodial $SU(2)_c$ -violation operator. Here, the operators $\mathcal{L}_{4,5}$ conserve $SU(2)_c$ while $\mathcal{L}_{6,7,10}$ violate $SU(2)_c$. The dependence on v and Λ is factorized out so that the dimensionless coefficient ℓ_n of the operator \mathcal{L}_n is naturally of $O(1)$ [12]. Because they contain *only* QGBCs these five operators cannot be directly tested via their tree-level contributions at low energies and are therefore least constrained from the current data. So far, only some rough estimates have been made by inserting them into the one-loop corrections and keeping the log-terms only². Here is a recent

¹⁾ It is advised that whenever the decoupling theorem [10] becomes ineffective, the nonlinear realization should better apply.

²⁾ The ignored constant contributions plus the new loop counter-terms are of the same order of magnitude as the log-terms. So, some uncertainties (like a factor of 2 to 3) may naturally exist in these estimates.

estimate at 90% C.L. by choosing $\Lambda = 2$ TeV and setting only one parameter nonzero at a time [30,15]:

$$\begin{aligned} -4 \leq \ell_4 &\leq 20, & -10 \leq \ell_5 &\leq 50; \\ -0.7 \leq \ell_6 &\leq 4, & -5 \leq \ell_7 &\leq 26, & -0.7 \leq \ell_{10} &\leq 3. \end{aligned} \quad (2)$$

(2) shows that the bounds on the $SU(2)_c$ symmetric parameters $\ell_{4,5}$ are about an order of magnitude above their natural size of $O(1)$; while the allowed range for the $SU(2)_c$ -breaking parameters ℓ_{6-10} is about a factor of $O(10-100)$ larger than that for $\ell_0 = \frac{\Lambda^2}{2v^2} \Delta\rho$ ($= \frac{\Lambda^2}{2v^2} \alpha T$) derived from the ρ (or T) parameter: $0.052 \leq \ell_0 \leq 0.12$ [15], for the same Λ and confidence level. To directly test the EWSB dynamics, it is crucial to probe these QGBCs at future high energy scattering processes where their contributions can be greatly enhanced due to the sensitive power-dependence on the scattering energy [15].

2. Quartic Gauge Boson Interactions and Underlying Models

So far the full theory underlying this effective EWCL is not determined, it is thus important to analyze how the typical resonance/non-resonance models contribute to these EWSB parameters. Knowing the theoretical sizes and patterns of these parameters tells how to use the phenomenological bounds derived in following sections for discriminating different new physics models. We mainly focus on the quartic gauge boson interactions (1) and consider [17] typical models such as a heavy scalar (S), a vector (V_μ^a) and an axial vector (A_μ^a) for the resonance scenario, and the new heavy doublet fermions for the non-resonance scenario.

• **A Non-SM Singlet Scalar** Up to dimension-4 and including both $SU(2)_c$ conserving and breaking effects, we write down the most general Lagrangian for a singlet scalar which is invariant under the SM gauge group $SU(2)_L \otimes U(1)_Y$:

$$\begin{aligned} \mathcal{L}_{\text{eff}}^S &= \frac{1}{2} \left[\partial^\mu S \partial_\mu S - M_S^2 S^2 \right] - V(S) \\ &\quad - \left[\frac{\kappa_s}{2} v S + \frac{\kappa'_s}{4} S^2 \right] \text{Tr} [\mathcal{V}_\mu \mathcal{V}^\mu] - \left[\frac{\tilde{\kappa}_s}{2} v S + \frac{\tilde{\kappa}'_s}{4} S^2 \right] [\text{Tr} \mathcal{T} \mathcal{V}_\mu]^2 \end{aligned} \quad (3)$$

where $V(S)$ only contains Higgs self-interactions. The SM Higgs boson corresponds to a special parameter choice: $\kappa_s = \kappa'_s = 1$, $\tilde{\kappa}_s = \tilde{\kappa}'_s = 0$ and $V(S) = V(S)_{\text{SM}}$. A heavy scalar can be integrated out from low energy spectrum and the corresponding contributions to (1) are derived as:

$$\ell_4^s = 0, \quad \ell_5^s = \frac{\kappa_s^2}{8} \geq 0; \quad \ell_6^s = 0, \quad \ell_7^s = \frac{\kappa_s \tilde{\kappa}_s}{4}, \quad \ell_{10}^s = \frac{\tilde{\kappa}_s^2}{8} \geq 0. \quad (4)$$

In (4), the deviation from $\kappa_s = 1$ and $\tilde{\kappa}_s = 0$ signals a *non-SM Higgs boson*.

• **Vector and Axial-Vector Bosons** The S -parameter measurement at LEP disfavors the naive QCD-like dynamics for the EWSB [11], where the vector ρ_{TC} is the lowest new resonance in the TeV regime. This suggests a necessity of including the axial-vector boson [18] in a general formalism for modeling the non-QCD-like dynamics. We consider the vector V_μ^a and axial-vector A_μ^a fields as the weak isospin triplets of custodial $SU(2)_c$. $\{V, A\}$ transform under the SM global $SU(2)_c$ as $\hat{V}_\mu \Rightarrow \hat{V}'_\mu = \Sigma_v \hat{V}_\mu \Sigma_v^\dagger$, $\hat{A}_\mu \Rightarrow \hat{A}'_\mu = \Sigma_v \hat{A}_\mu \Sigma_v^\dagger$, where $\hat{V}_\mu \equiv V_\mu^a \tau^a/2$, $\hat{A}_\mu \equiv A_\mu^a \tau^a/2$, and $\Sigma_v \in SU(2)_c$. If $\{V, A\}$ are further regarded as gauge fields of a new local hidden symmetry group $\mathcal{H} = SU(2)_L' \otimes SU(2)_R'$ (with a discrete left-right parity) [18], we can write down the following general Lagrangian (up to two derivatives), in the *unitary gauge* of the group \mathcal{H} ³ and with both $SU(2)_c$ -conserving and -breaking effects included⁴,

$$\mathcal{L}_{\text{eff}}^{VA} = \mathcal{L}_{\text{kinetic}}^{VA} - v^2 \left[\kappa_0 \text{Tr} \bar{V}_\mu^2 + \kappa_1 \text{Tr} (J_\mu^V - 2V_\mu)^2 + \kappa_2 \text{Tr} (J_\mu^A + 2A_\mu)^2 + \kappa_3 \text{Tr} A_\mu^2 \right. \\ \left. + \tilde{\kappa}_0 [\text{Tr} \tilde{\mathcal{T}} \bar{V}_\mu]^2 + \tilde{\kappa}_1 [\text{Tr} \tilde{\mathcal{T}} (J_\mu^V - 2V_\mu)]^2 + \tilde{\kappa}_2 [\text{Tr} \tilde{\mathcal{T}} (J_\mu^A + 2A_\mu)]^2 + \tilde{\kappa}_3 [\text{Tr} \tilde{\mathcal{T}} A]^2 \right] \quad (5)$$

where

$$\begin{cases} J_\mu^V = J_\mu^L + J_\mu^R \\ J_\mu^A = J_\mu^L - J_\mu^R \end{cases} \quad \begin{cases} J_\mu^L = \xi^\dagger D_\mu^L \xi = \xi^\dagger (\partial_\mu \xi + W_\mu \xi) \\ J_\mu^R = \xi D_\mu^R \xi^\dagger = \xi (\partial_\mu \xi^\dagger + B_\mu \xi^\dagger) \end{cases}$$

and, by definition, $V_\mu \equiv i\tilde{g}\hat{V}_\mu = i\tilde{g}V_\mu^a \tau^a/2$, $A_\mu \equiv i\tilde{g}\hat{A}_\mu = i\tilde{g}A_\mu^a \tau^a/2$, $\bar{V}_\mu \equiv U^\dagger D_\mu U = U^\dagger \mathcal{V}_\mu U$, $\tilde{\mathcal{T}} = \tau^3 = U^\dagger \mathcal{T} U$, and $U \equiv \xi^2$. Here \tilde{g} is the gauge coupling of the group \mathcal{H} . Among the above four new $SU(2)_c$ -conserving parameters κ_n 's, κ_0 is determined by normalizing the Goldstone kinematic term: $\kappa_0 = -4\kappa_2\kappa_3/(4\kappa_2 + \kappa_3)$. After eliminating the V and A fields in the heavy mass expansion, we derive ℓ_n 's below:

$$\begin{cases} \ell_4 = \ell_4^v + \ell_4^a \\ \ell_5 = \ell_5^v + \ell_5^a \\ \ell_6 = \ell_6^v + \ell_6^a \\ \ell_7 = \ell_7^v + \ell_7^a \\ \ell_{10} = \ell_{10}^v + \ell_{10}^a \end{cases} \quad \begin{cases} \ell_4^v = -\ell_5^v = 1/[2\sqrt{2}\tilde{g}v\Lambda^{-1}]^2 > 0 \\ \ell_4^a = -\ell_5^a = [\eta^2(\eta^2 - 2) + 16\tilde{\eta}^2]/[2\sqrt{2}\tilde{g}v\Lambda^{-1}]^2 \\ \ell_6^v = \ell_7^v = 0 \\ \ell_6^a = -\ell_7^a = -\tilde{\eta} [4(3 - \eta^2)\tilde{\eta} + (1 - \eta^2)\eta]/[2\sqrt{2}\tilde{g}v\Lambda^{-1}]^2 \\ \ell_{10}^v = \ell_{10}^a = 0 \end{cases} \quad (6)$$

in which

$$\eta = \frac{4\kappa_2}{4\kappa_2 + \kappa_3}, \quad \tilde{\eta} = \frac{2\kappa_2 + 4\tilde{\kappa}_2}{(4\kappa_2 + \kappa_3) + 2(4\tilde{\kappa}_2 + \tilde{\kappa}_3)} - \frac{2\kappa_2}{4\kappa_2 + \kappa_3}, \quad (7)$$

³⁾ By “unitary gauge” we mean a gauge containing no new Goldstone boson other than the three ones for generating the longitudinal components of the *known* W, Z . In fact, it is not essentially necessary to introduce such a new local symmetry \mathcal{H} for $\{V, A\}$ [19] since \mathcal{H} has to be broken anyway and $\{V, A\}$ can be treated as matter fields [20]. The hidden local symmetry formalism is more restrictive on the allowed free-parameters (κ_n 's etc) due to the additional assumption about that new local group \mathcal{H} .

⁴⁾ In the literature [18], only the $SU(2)_c$ -conserving operators were given.

and $\Lambda = \min\{M_V, M_A\}$. After ignoring the SM gauge couplings g and g' , $\{M_V, M_A\} \simeq \{\tilde{g}v\sqrt{\kappa_1}, \tilde{g}v\sqrt{\kappa_2 + \kappa_3/4}\}$, at the leading order. In (6), the factor $1/[\tilde{g}v\Lambda^{-1}]^2 \simeq \kappa_1(\Lambda/M_V)^2 = O(\kappa_1)$ and all $SU(2)_c$ -breaking terms depend on $\tilde{\eta}$. Note that the $SU(2)_c$ -symmetric contribution from the axial-vector boson interactions to $\ell_4^a = -\ell_5^a$ becomes negative for $|\eta| < \sqrt{2}$, while the summed contribution $\ell_4 = -\ell_5 = [(\eta^2 - 1)^2 + 16\tilde{\eta}^2]/[2\sqrt{2}\tilde{g}v\Lambda^{-1}]^2 \geq 0$. The deviation of η and/or $\tilde{\eta}$ from $\eta(\tilde{\eta}) = 0$ represents the *non-QCD-like* EWSB dynamics.

• **Heavy Doublet Fermions** Take for instance a model of one flavor heavy chiral fermions which form a left-handed weak doublet $(U_L, D_L)^T$ and right-handed singlets $\{U_R, D_R\}$, and joins a new strong $SU(N)$ gauge group in its fundamental representation. Their small mass-splitting breaks the $SU(2)_c$ and is characterized by the parameter $\omega = 1 - [M_U/M_D]^2$. The anomaly-cancellation is ensured by assigning the $\{U, D\}$ electric charges as $\{+\frac{1}{2}, -\frac{1}{2}\}$. By taking $\{U, D\}$ as the source of the EWSB, the W, Z masses can be generated by heavy fermion loops. The new contributions to the quartic gauge couplings of W/Z come from the *non-resonant* $\{U, D\}$ box-diagrams. The leading results in the $1/M_{U,D}$ and ω expansions are summarized below:

$$\ell_4^f = -2\ell_5^f = \left[\frac{\Lambda}{4\pi v} \right]^2 \frac{N}{12} > 0 ; \quad \ell_6^f = -\ell_7^f = - \left[\frac{\Lambda}{4\pi v} \right]^2 \frac{7N}{240} \omega^2 , \quad \ell_{10} = 0 ; \quad (8)$$

in which $\Lambda = \min\{M_U, M_D\}$.

3. A Global Analysis on Probing QGBCs versus TGBCs at the LHC

The general EWCL formalism [13] contains in total 15 NLO new operators whose coefficients (ℓ_n 's) depend on the details of the underlying dynamics as exemplified in the previous section. It is shown [15] that, except for $\ell_{0,1,8}$ (S, T, U), the current data only bound a few triple gauge boson couplings (TGBCs) to $O(10)$ at the 1σ -level and give no direct tree-level bound on QGBCs. The rough estimates of the bounds from 1-loop corrections still allow QGBCs to be of $O(5 - 50)$. For a *complete* test of the EWSB sector in discriminating different dynamical models, all these TGBCs and QGBCs (ℓ_n 's) have to be measured through various high energy VV -fusion and $f\bar{f}^{(\prime)}$ -annihilation processes. ($V^a = W^\pm, Z^0$.) For this purpose, a systematic global analysis [15] has been carried out which reveals the important overall physical pictures and guides us for further elaborate precise numerical studies (cf. Secs. 4-5). In performing such a global analysis we developed a precise electroweak power counting rule (à la Weinberg) for conveniently estimating *all* high energy scattering amplitudes and formulated the equivalence theorem (ET) [6] as a *necessary* physical criterion for sensitively probing the EWSB dynamics. Applying this counting method, we have carried out a systematic analysis for all $V^aV^b \rightarrow V^cV^d$ and $f\bar{f}^{(\prime)} \rightarrow V^aV^b, V^aV^bV^c$ processes by estimating the contributions to their S -matrix elements from both the

leading order operator up to one-loop and the other 15 NLO operators at the tree-level. Based upon the basic features of the chiral perturbation expansion, we further build the following electroweak power counting hierarchy for the S -matrix elements,⁵

$$\frac{E^2}{f_\pi^2} \gg \left[\frac{E^2 E^2}{f_\pi^2 \Lambda^2}, \, g \frac{E}{f_\pi} \right] \gg \left[g \frac{E}{f_\pi} \frac{E^2}{\Lambda^2}, \, g^2 \right] \gg \left[g^2 \frac{E^2}{\Lambda^2}, \, g^3 \frac{f_\pi}{E} \right] \gg \left[g^3 \frac{E f_\pi}{\Lambda^2}, \, g^4 \frac{f_\pi^2}{E^2} \right] \gg g^4 \frac{f_\pi^2}{\Lambda^2} . \quad (9)$$

In the typical TeV region, for $E \in (750 \text{ GeV}, 1.5 \text{ TeV})$, this gives:

$$(9.3, 37) \gg [(0.55, 8.8), (2.0, 4.0)] \gg [(0.12, 0.93), (0.42, 0.42)] \gg [(0.025, 0.099), (0.089, 0.045)] \gg [(5.3, 10.5), (19.0, 4.7)] \times 10^{-3} \gg (1.1, 1.1) \times 10^{-3} ,$$

where E is taken to be the invariant mass of the VV pair. This power counting hierarchy can be nicely understood. In (9), from left to right, the hierarchy is built up by increasing either the number of derivatives (i.e. power of E/Λ) or the number of external transverse gauge boson V_T 's (i.e. the power of gauge couplings). This power counting hierarchy provides us a theoretical base to classify all the relevant scattering amplitudes in terms of the three essential parameters E , f_π and Λ plus possible gauge/Yukawa coupling constants.

At the event-rate-level, we have adopted the usual leading-log effective vector boson method [24] to reasonably and conveniently estimate the VV -luminosities. In Fig. 1, the rate $|R_B|$ denotes an intrinsic background defined via the formulation of the ET as a necessary criterion for the sensitivities to the EWSB [6,15]. Fig. 1 shows that, at the 14TeV LHC with $\int \mathcal{L} = 100 \text{ fb}^{-1}$ Luminosity and for $\Lambda = 2 \text{ TeV}$, the W^+W^- -fusion is most sensitive to $\ell_{4,5}$ (QGBCs) and marginally sensitive to $\ell_{3,9,11,12}$; while the $q\bar{q}' \rightarrow W^+Z$ annihilation can best probe $\ell_{3,11,12}$ and marginally test $\ell_{8,9,14}$. Hence, the VV -fusions and $f\bar{f}^{(\prime)}$ -annihilations are *complementary* in probing the different sets of these NLO parameters (the QGBCs and TGBCs) at the LHC.

4. Measuring the QGBCs via WW -Fusion Processes

Though the LHC will give the first direct test on these new quartic gauge boson couplings (QGBCs), the large backgrounds limit its sensitivity and cutting off the backgrounds significantly reduces the event rate. As shown in Ref. [21], for the non-resonance $W^\pm W^\pm$ production channels in the TeV regime only around 10 signal events were predicted at the LHC with a 100 fb^{-1} annual luminosity after imposing necessary cuts in the gold-plated modes (by pure leptonic decays). The corresponding study at the TeV $e^\pm e^-$ LCs opens a more exciting possibility [22,23].

In this and next sections we review how to make further precision constraints for the QGBCs via the WW -fusion [25,26], WWZ/ZZZ -production [17]⁶, and their

⁵⁾ For $f\bar{f}^{(\prime)} \rightarrow VVV$ amplitudes, there is an additional factor $1/f_\pi$ by dimensional counting.

⁶⁾ The WWZ/ZZZ -production in the SM was first studied in Ref. [27], and later some analyses on including the anomalous couplings have also appeared [28] for the case of unpolarized e^\mp beams. For a very recent study similar to Ref. [17] for WWZ/ZZZ -production, see Ref. [30].

interplay at LCs [17,29], which is much cleaner than the LHC so that the final state W/Z 's can be detected via the dijet mode and with large branching ratios. Due to the limited calorimeter energy resolution, the misidentification probability of W versus Z and the rejection of certain fraction of diboson events should be considered [23]. Inclusion of the leptonic decay of Z to e^-e^+ and $\mu^-\mu^+$ is also useful. According to the study of Ref. [23], the (mis)identification probabilities of W and Z via jet-decay mode can be derived as

$$\begin{aligned} W &\Rightarrow 85\% \text{ } W, \text{ } 10\% \text{ } Z, \text{ } 5\% \text{ } \text{reject} , \\ Z &\Rightarrow 22\% \text{ } W, \text{ } 74\% \text{ } Z, \text{ } 4\% \text{ } \text{reject} . \end{aligned} \quad (10)$$

The detection efficiencies for WW , ZZ and WZ final states are thus estimated below, which are about 34%:

$$\begin{aligned} \epsilon_{WW} &= [0.68 \times 0.85]^2 = 33.4\% , \quad \epsilon_{ZZ} = [0.70 \times 0.74 + 0.067]^2 = 34.2\% , \\ \epsilon_{WZ} &= [0.68 \times 0.85][0.70 \times 0.74 + 0.067] = 33.8\% . \end{aligned} \quad (11)$$

To completely determine all the QGBCs, we need at least five independent processes. From WW -fusions alone, we can have

Full process :	Sub – process :	Relevant parameter :
$e^-e^+ \rightarrow \nu\bar{\nu}W^-W^+$,	$(W^-W^+ \rightarrow W^-W^+)$,	$(\ell_{4,5})$,
$e^-e^- \rightarrow \nu\bar{\nu}W^-W^-$,	$(W^-W^- \rightarrow W^-W^-)$,	$(\ell_{4,5})$;
$e^-e^+ \rightarrow \nu\bar{\nu}ZZ$,	$(W^-W^+ \rightarrow ZZ)$,	$(\ell_{4,5}; \ell_{6,7})$,
$e^-e^+ \rightarrow e^\pm\nu W^\mp Z$,	$(W^\mp Z \rightarrow W^\mp Z)$,	$(\ell_{4,5}; \ell_{6,7})$,
$e^-e^+ \rightarrow e^-e^+ZZ$,	$(ZZ \rightarrow ZZ)$,	$([\ell_4 + \ell_5] + 2[\ell_6 + \ell_7 + \ell_{10}])$;

where in the round brackets the corresponding fusion (signal) sub-processes are given. We see that $\ell_{4,5}$ can be cleanly tested via the first two processes in (12), as shown by Fig. 2. (All our plots have chosen the new physics cutoff as $\Lambda = 2$ TeV and the numerical results for other values of Λ can be obtained via re-scaling.) By including the third and fourth reactions $\ell_{6,7}$ can be further disentangled. Finally the fifth channel provides a unique probe on ℓ_{10} . Though this scheme is complete in principle, the realistic situation is more involved. Note that the rate of the last reaction in (12) is significantly lower than all others due to the double suppressions of the e - e - Z couplings while the fourth channel has huge backgrounds which are uneasy to overcome [23,26]. But $ZZ \rightarrow ZZ$ also has an advantage due to the absence fusion-type backgrounds and the triple gauge boson couplings have no contribution either. This makes it relatively cleaner than others. Since the parameter ℓ_{10} appears only in $4Z$ vertex, the above last channel has to be used anyway when only the fusion mechanism is studied. (For the process $e^-e^+ \rightarrow ZZZ$ on ℓ_{10} , see Sec. 5.) Since the large backgrounds make the WZ -channel less useful (see Fig. 4a below), we propose to use the production $e^-e^+ \rightarrow WWZ$ (cf. Sec. 5) to complete this five parameter determination.

From the above analysis, we finally summarize below the 90% C.L. (one-parameter) fusion-bounds for $\Lambda = 2$ TeV at a later stage of the LC with the energy $\sqrt{s} = 1.6$ TeV and the integrated luminosity $\int \mathcal{L} = 200$ fb^{-1} :

$$\begin{aligned} -0.13 &\leq \ell_4 \leq 0.10, & -0.08 &\leq \ell_5 \leq 0.06; \\ -0.22 &\leq \ell_6 \leq 0.22, & -0.12 &\leq \ell_7 \leq 0.10, & -0.21 &\leq \ell_{10} \leq 0.21; \end{aligned} \quad (13)$$

which are very stringent. Here we have used a 90% (65%) polarization for the $e^- (e^+)$ beam.

5. WWZ/ZZZ -Production and its Interplay with WW -Fusion

To probe the QGBCs (1), we know [15] that the WW -fusion amplitudes have the highest E -power dependence in the TeV regime while the s -channel signals of the WWZ/ZZZ -production lose an enhancement factor of $(E/v)^2$ relative to that of the fusion processes. When the collider energy is reduced by half (from 1.6 TeV down to 800 GeV), the sensitivity of the WW -fusion decreases by about a factor of 20 or more [25,26]. We thus expect that $ee \rightarrow WWZ, ZZZ$ become more important at the earlier phase of the LCs and will be competitive with and complementary to the fusion processes for the later stages of the LCs around $0.8 \sim 1$ TeV [17]. In fact, it was revealed that even at the 1.5/1.6 TeV, $e^+e^- \rightarrow WWZ$ plays a crucial role in achieving a clean five-parameter analysis [17,29].

To avoid the potential fusion backgrounds from $e^-e^+ \rightarrow eeZZ, eeWW$, we now only add the $Z \rightarrow \mu^-\mu^+$ decay besides the dijet-decay mode. The detection efficiencies for ZZZ and WWZ final states are thus estimated to be about 16.8% and 18.4%, respectively. It turns out that $e^-e^+ \rightarrow WWZ$ has huge backgrounds due to the t -channel ν_e or $e-\nu_e$ exchange, and the kinematic cuts alone help very little. However, we find that such type of backgrounds involve the left-handed W - e - ν coupling and thus can be effectively suppressed by using the right(left)-hand polarized $e^- (e^+)$ beam. The highest sensitivity is reached by maximally polarizing *both* e^- and e^+ beams. The crucial roles of the beam polarization and the higher collider energy for the WWZ -production are demonstrated in Fig. 3a, where $\pm 1\sigma$ exclusion contours for ℓ_4 - ℓ_5 are displayed at $\sqrt{s} = 0.5, 0.8, 1.0$ and 1.6 TeV, respectively. The beam polarization has much less impact on the ZZZ mode, due to the almost axial-vector type e - Z - e coupling. Including the same polarizations as in the case of the WWZ mode, we find about 10 – 20% improvements on the bounds from the ZZZ -production. Assuming the two beam polarizations (90% e^- and 65% e^+), we summarize the final $\pm 1\sigma$ bounds for both ZZZ and WWZ channels and their combined 90% C.L. contours for 0.5 TeV with $\int \mathcal{L} = 50$ fb^{-1} in Fig. 3b (representing the *first direct probe* at the LC) and for 1.6 TeV with $\int \mathcal{L} = 200$ fb^{-1} in Fig. 3c (representing the *best sensitivity* gained from the final stage of the LC with energy around 1.5/1.6 TeV). Note that, the 90% C.L. level bounds on ℓ_4 - ℓ_5 at 0.5 TeV are within $O(10-20)$, while at 1.6 TeV they sensitively reach $O(1)$. The WWZ channel gives the same bounds for ℓ_4 - ℓ_5 and

ℓ_6 - ℓ_7 , while the ZZZ channel imposes stronger bound on ℓ_6 - ℓ_7 due to a factor of 2 enhancement from the $4Z$ -vertex. ℓ_{10} only contributes to ZZZ final state and can be probed at the similar level.

For comparison, a parallel analysis to Fig. 3b-c is further performed for the case without e^+ -beam polarization (but with e^- polarization the same as before). For a two-parameter ($\ell_{4,5}$) study, the results are listed below at 90% C.L.:

$$\begin{aligned} \text{at 0.5 TeV : } & -12 (-18) \leq \ell_4 \leq 21 (27), & -17 (-22) \leq \ell_5 \leq 9.5 (15); \\ \text{at 1.6 TeV : } & -0.50 (-0.67) \leq \ell_4 \leq 1.5 (1.7), & -1.3 (-1.5) \leq \ell_5 \leq 0.36 (0.58); \end{aligned} \quad (14)$$

where the numbers in the parentheses denote the bounds from polarizing the e^- -beam alone. The comparison in (14) shows that without e^+ -beam polarization, the sensitivity will decrease by about 15% – 60%. Therefore, making use of the possible e^+ -beam polarization with a degree around 65% is clearly helpful. In the above, the total rates are used to derive the numerical bounds. We have further studied the possible improvements by including different characteristic distributions, but no significant increase of the sensitivity is found.

Now, we are ready to analyze the interplay with WW -fusion processes. As noted in Sec. 4, the WZ -channel in (12) has large γ -induced $eeWW$ background in which one e is lost in the beam-pipe and one W misidentified as Z . A cut on the missing $p_\perp(\nu)$ is imposed to specially suppress this background. Even though, the final sensitivity still turns out to be less useful in constraining the ℓ_6 - ℓ_7 plane (cf. Fig. 4a) [26]. To sensitively bound $\{\ell_6, \ell_7\}$ (especially ℓ_6) well below $O(1)$, we propose to use the production $e^-e^+ \rightarrow WWZ$. Fig. 4a demonstrates the interplay of WW -fusion and WWZ -production for discriminating the $SU(2)_c$ -breaking QGBCs ℓ_6 - ℓ_7 at $\sqrt{s} = 1.6$ TeV. The ZZZ -production can also bound ℓ_{10} , in addition to the $eeZZ$ fusion-channel in (12). Assuming that $\ell_{4,5;6,7}$ are constrained by the processes mentioned above, we set their values to the reference point (zero) for simplicity and define the statistic significance $S = |\mathcal{N} - \mathcal{N}_0|/\sqrt{\mathcal{N}_0}$ which is a function of ℓ_{10} . Here \mathcal{N} is the total event-number while \mathcal{N}_0 is the number at $\ell_{10} = 0$. As shown in Fig. 4b, at 1.6 TeV, the sensitivity of $e^-e^+ \rightarrow eeZZ$ for probing ℓ_{10} is better than that of $e^-e^+ \rightarrow ZZZ$.

In summary, the first direct probe on these QGBCs will come from the early phase of the LC at 500 GeV, where the WW -fusion processes are not useful. The two mechanisms become more competitive and complementary at energies $\sqrt{s} \sim 0.8 - 1$ TeV. From (13) and Table 1, we see that at a later stage of the LC with $\sqrt{s} = 1.6$ TeV, the 90% C.L. one-parameter bounds on $\ell_{4,5}$ from WWZ/ZZZ -modes are about a factor of $3 \sim 6$ weaker than that from WW -fusions; while the bounds on $\ell_{6,7,10}$ are comparable. In a complete multi-parameter analysis, the WWZ -channel is crucial for determining ℓ_6 - ℓ_7 even at a 1.6 TeV LC (cf. Fig. 4a).

Table 1: Combined 90% C.L. bounds on ℓ_{4-10} from WWZ/ZZZ -production. For simplicity, we set one parameter to be nonzero at a time. The bound on ℓ_{10} comes from

ZZZ -channel alone.

\sqrt{s} (TeV)	0.5	0.8	1.0	1.6
$\int \mathcal{L}$ (fb $^{-1}$)	50	100	100	200
WWZ/ZZZ	$-9.5 \leq \ell_4 \leq 11.7$	$-2.7 \leq \ell_4 \leq 3.2$	$-1.7 \leq \ell_4 \leq 2.0$	$-0.50 \leq \ell_4 \leq 0.58$
Bounds (at 90% C.L.)	$-9.8 \leq \ell_5 \leq 8.9$ $-5.0 \leq \ell_6 \leq 5.8$ $-5.0 \leq \ell_7 \leq 5.7$ $-4.3 \leq \ell_{10} \leq 5.2$	$-3.1 \leq \ell_5 \leq 2.3$ $-1.5 \leq \ell_6 \leq 1.6$ $-1.5 \leq \ell_7 \leq 1.5$ $-1.4 \leq \ell_{10} \leq 1.4$	$-1.9 \leq \ell_5 \leq 1.4$ $-0.95 \leq \ell_6 \leq 1.0$ $-0.95 \leq \ell_7 \leq 0.92$ $-0.83 \leq \ell_{10} \leq 0.88$	$-0.54 \leq \ell_5 \leq 0.36$ $-0.28 \leq \ell_6 \leq 0.28$ $-0.28 \leq \ell_7 \leq 0.26$ $-0.26 \leq \ell_{10} \leq 0.26$
Range of $ \ell_n $	$\leq O(4 \sim 10)$	$\leq O(1 \sim 3)$	$\leq O(0.8 \sim 2)$	$\leq O(0.3 \sim 0.6)$

6. Concluding Remarks

Despite the constantly increasing evidence in supporting the Standard Model (SM) over the past 30 years, we particle physicists have been struggling in search for *New Physics Beyond the SM* so far [2,3]. Among the numerous ways for going beyond the SM, the Higgs boson hypothesis [31] stands out. The updated direct Higgs search at LEP [2] puts a 95% C.L. lower bound $m_H \geq 89.3$ GeV. Due to the discrepancy between the precision Z -decay asymmetry measurement and the direct Higgs search limit, the combined 95% C.L. upper Higgs mass bound from the global fit has been shown to significantly increase toward the TeV regime [4]. However, the unitarity [32] and triviality [33] theoretically forbid the SM Higgs mass to go beyond the TeV scale, at which we are facing an exciting strong electroweak symmetry breaking (EWSB) dynamics. Below the new heavy resonance, we have to first probe the EWSB parameters formulated by means of the electroweak chiral Lagrangian (EWCL), among which the quartic gauge boson interactions penetrate the pure Goldstone dynamics. After commenting upon the low energy indirect bounds and analyzing the different patterns of these quartic couplings predicted by the typical resonance/non-resonance models, we estimate the sensitivity of the LHC to probing these couplings, and then analyze the constraints on them via WWZ/ZZZ -production and WW -fusion at the next generation $e^\pm e^-$ linear colliders (LCs). The interplay of the two production mechanisms and the important role of the beam-polarization at the LCs are revealed and stressed.

Finally, we remark that the same physics may be similarly and better studied at a multi-TeV muon collider (MTMC) ($\sqrt{s} \simeq 3 - 4$ TeV) with high luminosity ($\sim 500 - 1000$ fb $^{-1}$ /year) [34,35]. Due to the higher center mass energy of the MTMC, certain unitarization on the EWCL is needed for studying the WW -fusions. The

other muon collider options, like $\mu^-\mu^-$ and $\mu^+\mu^+$ are likely to be as easily achieved as $\mu^-\mu^+$ mode. Furthermore, the large muon mass relative to the electron mass makes the initial state photon-radiation of the muon collider much less severe than that of the electron collider. The two drawbacks of a muon collider in comparison with an electron linear collider are [35]: (i) substantial beam polarization ($\geq 50\%$) can be achieved only with a significant sacrifice in luminosity; (ii) the $\gamma\gamma$ and $\mu\gamma$ options are probably not very feasible.

Acknowledgments

I am grateful to the working group convener Tao Han for invitation and FermiLab for hospitality. Special thanks go to Tao Han and C.-P. Yuan for carefully reading the draft and providing many useful suggestions. I thank them and all other collaborators, E. Boos, W. Kilian, Y.-P. Kuang, A. Pukhov and P.M. Zerwas, for productive collaborations [15,26,17] upon which this review is based. I am also indebted to K. Floettmann and R. Frey for discussing the e^\mp -beam polarizations, and many other colleagues such as M.S. Chanowitz, R. Casalbuoni, D. Dominici, K. Hagiwara, K. Hikasa, G. Jikia, I. Kuss, A. Likhoded, C.R. Schmidt and G. Valencia for useful conversations on this subject. This work is supported by the U.S. Natural Science Foundation.

References

1. J. Goldstone, Nuovo Cim. **19** (1961) 154.
2. C. Rembser, *Recent Results on LEP2*, plenary talk at International Symposium on “Frontiers of Phenomenology from Non-perturbative QCD to New Physics”, March 23-26, 1998, Madison, Wisconsin.
3. B.C. Allanach et al, *Report of the Working Group on ‘Searches’*, hep-ph/9708250; A. Sopczak, *Searches for Higgs Bosons at LEP2*, hep-ph/9712283; and references therein.
4. M.S. Chanowitz, Phys. Rev. Lett. (1998), in press, and hep-ph/9710308.
5. J.M. Cornwall, D.N. Levin, and G. Tiktopoulos, Phys. Rev. **D10** (1974) 1145; B.W. Lee, C. Quigg, and H. Thacker, Phys. Rev. **D16** (1977) 1519; M.S. Chanowitz and M.K. Gaillard, Nucl. Phys. **B261** (1985) 379. G.J. Gounaris, R. Kögerler, and H. Neufeld, Phys. Rev. **D34** (1986) 3257; Y.-P. Yao and C.-P. Yuan, Phys. Rev. **D38** (1988) 2237.
6. H.-J. He, Y.-P. Kuang, C.-P. Yuan, Phys. Rev. **D51** (1995) 6463; H.-J. He and W.B. Kilgore, Phys. Rev. **D55** (1997) 1515; H.-J. He, Y.-P. Kuang, and X. Li, Phys. Rev. Lett. **69** (1992) 2619; Phys. Rev. **D49** (1994) 4842; Phys. Lett. **B329** (1994) 278; and references therein.
7. E. Accomando et al, *Physics with e^+e^- Linear Colliders*, (ECFA/DESY LC Physics Working Group), Phys. Rep. (1998), in press and DESY-97-100 (hep-ph/9705442); H. Murayama and M.E. Peskin, Ann. Rev. Nucl. & Part. Sci. **46** (1996) 533.
8. K. Hikasa, *Physics at Linear Colliders*, plenary talk at International Symposium on “Frontiers of Phenomenology from Non-perturbative QCD to New Physics”, March 23-26, 1998, Madison, Wisconsin.
9. M.E. Peskin, Prog. Theor. Phys. Suppl. **123** (1996) 507; H.E. Haber, hep-ph/9703381; G.L. Kane, hep-ph/9709318; and references therein.
10. T. Appelquist and J. Carazzone, Phys. Rev. **D11** (1975) 2856.
11. M. Peskin, Talk at the Snowmass Conference (June, 1996), and the working group summary report, hep-ph/9704217.
12. For a nice review, H. Georgi, Ann. Rev. Nucl. & Part. Sci. **43** (1994) 209.
13. T. Appelquist and C. Bernard, Phys. Rev. **D22** (1980) 200; A.C. Longhitano, Nucl. Phys. **B188** (1981) 118; T. Appelquist and G.-H. Wu, Phys. Rev. **D48** (1993) 3235; J. Bagger, S. Dawson, and G. Valencia, Nucl. Phys. **B399** (1993) 364; and references therein.
14. S. Weinberg, Physica **96A** (1979) 327.
15. H.-J. He, Y.-P. Kuang, and C.-P. Yuan, hep-ph/9708402; Phys. Rev. **D55** (1997) 3038, Mod. Phys. Lett. **A11** (1996) 3061; Phys. Lett. **B382** (1996) 149; for an updated comprehensive review, hep-ph/9704276 and DESY-97-056, Lectures in the Proceedings of the CCAST (World Laboratory) Workshop on *Physics at TeV Energy Scale*, Vol. 72, pp.119-234.
16. O.J.P. Eboli et al., Phys. Lett. **B375** (1996) 233; **B339** (1995) 119; S. Dawson and G. Valencia, Nucl. Phys. **B439** (1995) 3.
17. T. Han, H.-J. He, and C.-P. Yuan, Phys. Lett. **B422** (1998) 294 and hep-

ph/9711429.

18. R. Casalbuoni, et al, Phys. Rev. **D53** (1996) 5201; D. Dominici, hep-ph/9711385; and references therein.
19. H. Georgi, Nucl. Phys. **B331** (1990) 311.
20. C.G. Callan, S. Coleman, J. Wess, B. Zumino, Phys. Rev. **177** (1969) 2247.
21. J. Bagger, V. Barger, K. Cheung, J. Gunion, T. Han, G.A. Ladinsky, R. Rosenfeld, and C.-P. Yuan, Phys. Rev. **D49** (1994) 1246; **D52** (1995) 3878.
22. K. Hagiwara, private communications; K. Hagiwara, J. Kanzaki, and H. Murrayama, KEK-TH-282, 1991.
23. V. Barger, K. Cheung, T. Han, R.J.N. Phillips, Phys. Rev. **D52** (1995) 3815.
24. M.S. Chanowitz and M.K. Gaillard, *Phys. Lett.* **B142**, 85 (1984); G.L. Kane, W.W. Repko and W.R. Rolnick, *ibid.* **B148**, 367 (1984); S. Dawson, *Nucl. Phys.* **B249**, 427 (1985).
25. H.-J. He, DESY-97-037, in the proceedings of “*The Higgs Puzzle*”, pp.207-217, Ringberg, Munich, Germany, December 8-13, 1996, Ed. B. Kniehl, (World Scientific Pub).
26. E. Boos, H.-J. He, W. Kilian, A. Pukhov, C.-P. Yuan, and P.M. Zerwas, Phys. Rev. **D57** (1998) 1553 and hep-ph/9708310.
27. V. Barger and T. Han, Phys. Lett. **B212** (1988) 117;
V. Barger, T. Han, and R.J.N. Phillips, Phys. Rev. **D39** (1989) 146.
28. G. Belanger and F. Boudjema, Phys. Lett. **B288** (1992) 201;
S. Dawson, A. Likhoded, G. Valencia, and O. Yuschenko, hep-ph/9610299.
29. H.-J. He, DESY-97-140, in the proceedings of 5th International Conference on “*Physics Beyond the Standard Model*”, Balholm, Norway, April 29-May 4, 1997, pp.474-481, ed. G. Eigen, P. Osland, and B. Stugu, (American Physical Institute Pub).
30. O.J.P. Eboli, M.C. Gonzalez-Garcia, and J.K. Mizukoshi, hep-ph/9711499.
31. P.W. Higgs, Phys. Lett. **12** (1964) 132; Phys. Rev. Lett. **13** (1964) 508; F. Englert and R. Brout, Phys. Rev. Lett. **13** (1964) 321; G.S. Guralnik, C.R. Hagen, and T.W.B. Kibble, Phys. Rev. Lett. **13** (1964) 585.
32. D.A. Dicus and V.S. Mathur, Phys. Rev. **D7** (1973) 3111; M. Veltman, Acta. Phys. Pol. **B8** (1977) 475; B.W. Lee, C. Quigg, and H. Thacker, Phys. Rev. **D16** (1977) 1519; M.S. Chanowitz and M.K. Gaillard, Nucl. Phys. **B261** (1985) 379.
33. R. Dashen and H. Neuberger, Phys. Rev. Lett. **50** (1983) 1897; J. Kuti, L. Lin and Y. Shen, Phys. Rev. Lett. **61** (1988) 678; M. Lüscher and P. Weisz, Nucl. Phys. **B318** (1989) 705.
34. V. Barger, M. Berger, J. Gunion and T. Han, Phys. Rev. **D55** (1997) 142.
35. J. Gunion, in these proceedings and hep-ph/9802258;
V. Barger, M. Berger, J. Gunion and T. Han, hep-ph/9604334 and hep-ph/9704290.

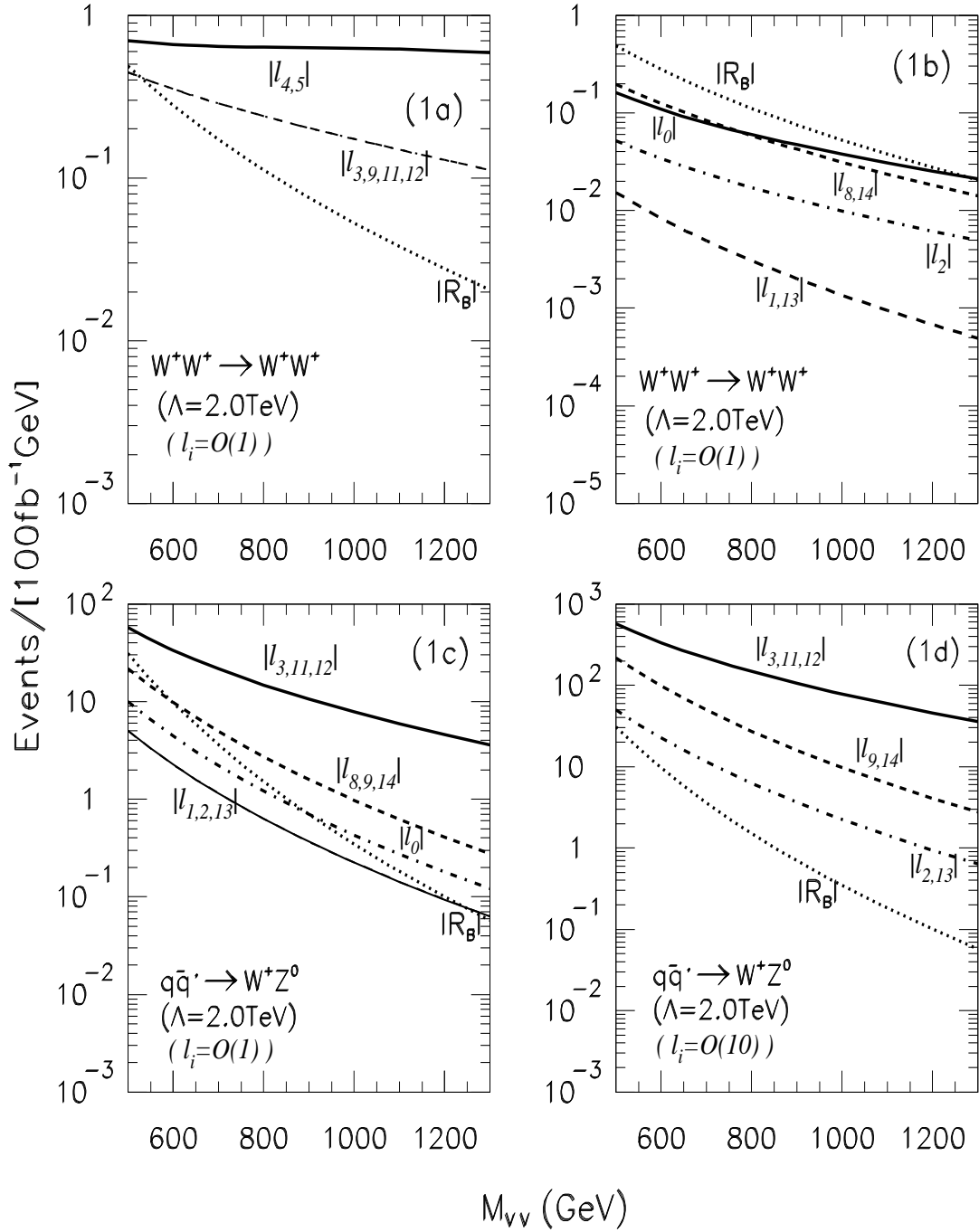


FIGURE 1. A classification of the contributions from all 15 next-to-leading order operators at the 14 TeV LHC (with 100 fb^{-1} annual luminosity) for $\Lambda = 2 \text{ TeV}$.

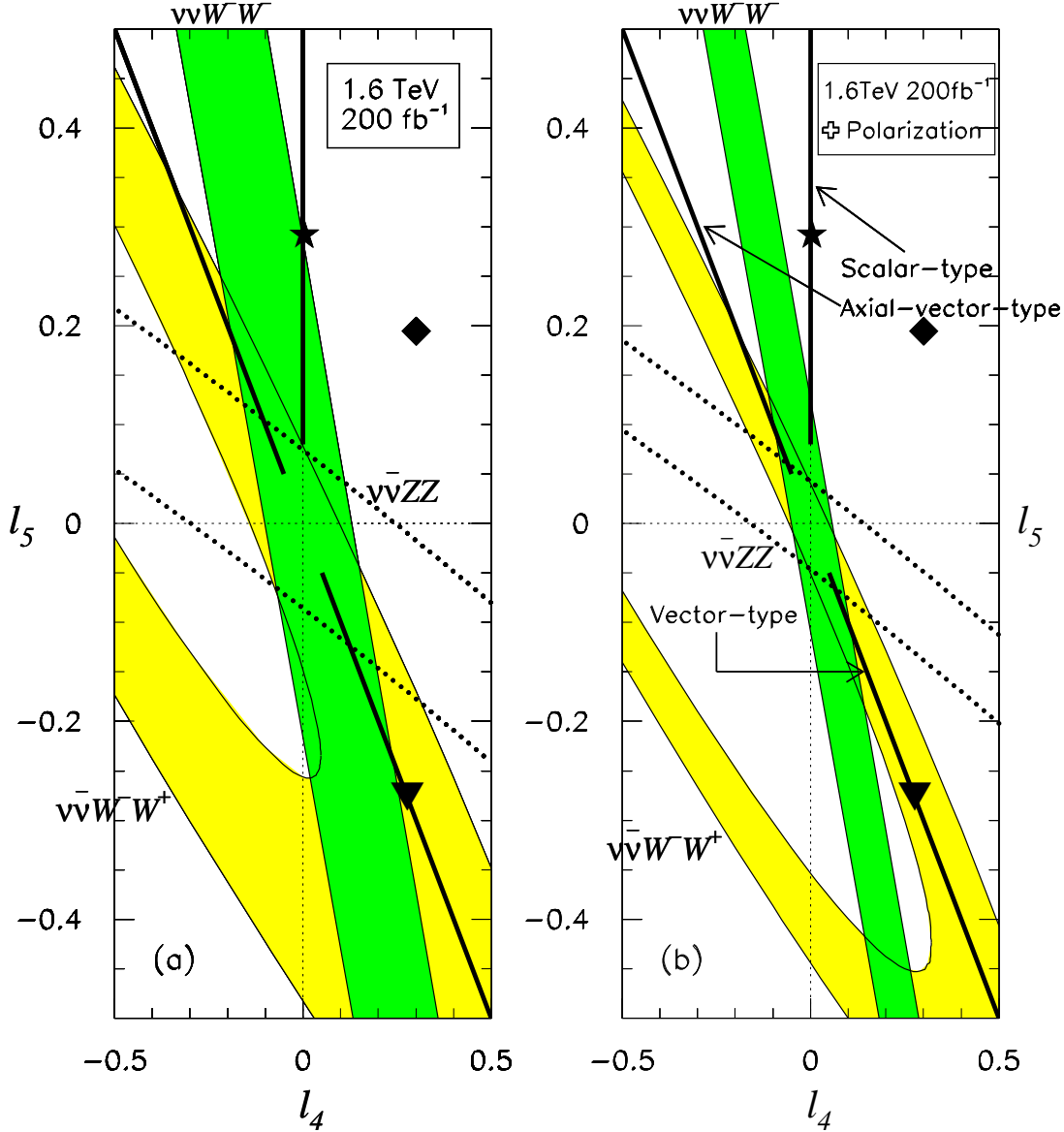


FIGURE 2. Determining the $SU(2)_c$ -symmetric parameters ℓ_4 - ℓ_5 at 1.6 TeV e^-e^+ / e^-e^- LCs. Here the $\pm 1\sigma$ exclusion contours are displayed. (a). unpolarized case; (b). the case with 90%(65%) polarized e^- (e^+) beam. Contributions from three types of resonance models (scalar, vector and axial-vector) to (ℓ_4, ℓ_5) are shown by the thick solid lines. The different points on these solid lines correspond to different values of their couplings to the weak gauge bosons. Note that for axial-vector-type, it is also possible to have $\ell_4 + \ell_5 = 0$ with $\ell_4 \geq 0$, i.e., similar to the vector-type case. This makes the discrimination more involved. Big-star: from a scalar; black-triangle-down: from a vector; black-lozenge: from mixed contributions of a heavy scalar and vector. (Here we typically set these heavy resonances around 2 TeV.)

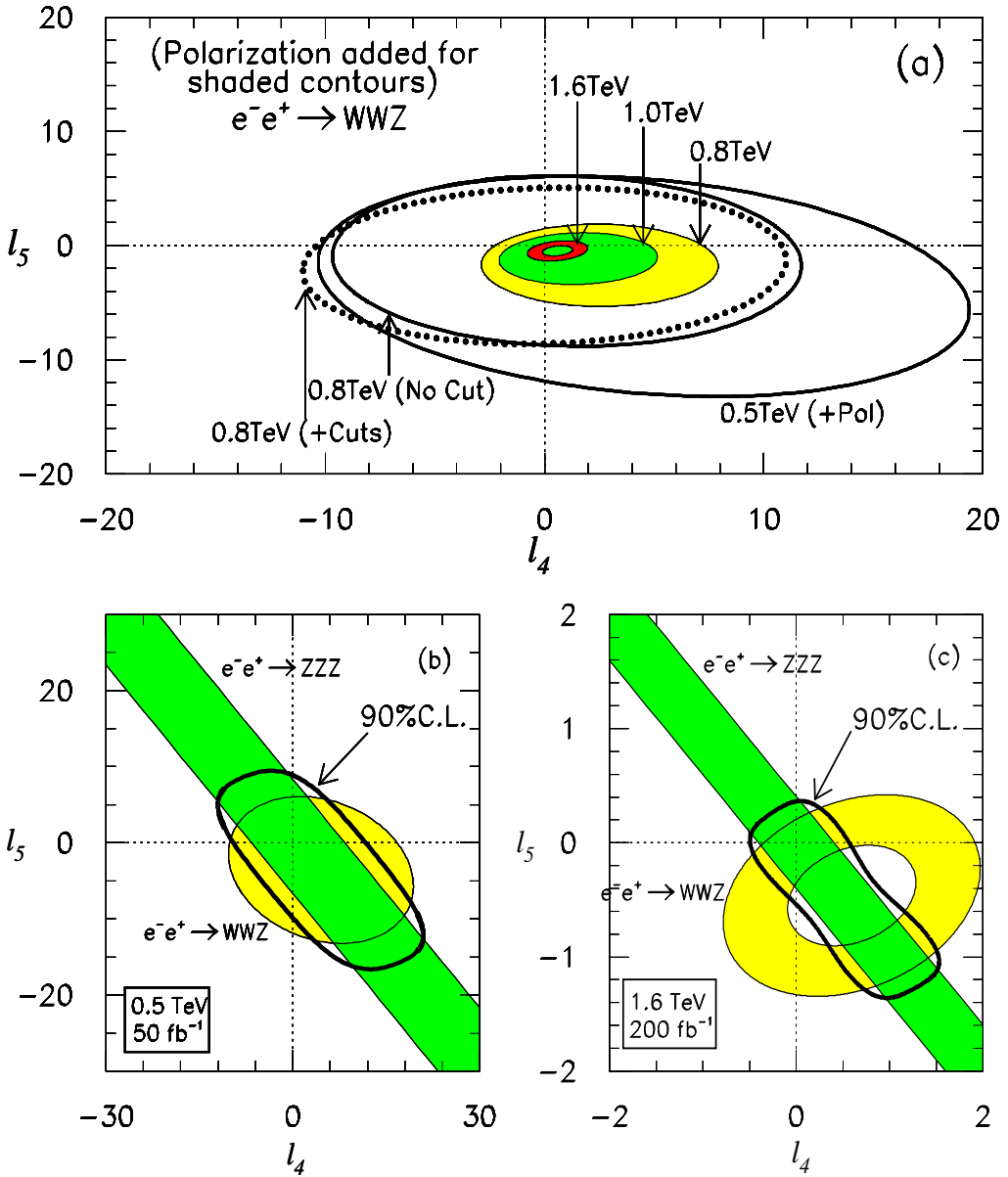


FIGURE 3. Probing ℓ_4 - ℓ_5 via WWZ and ZZZ production processes. The roles of the polarization and the higher collider energy for $e^-e^+ \rightarrow WWZ$ are shown by the $\pm 1\sigma$ exclusion contours in (a). The integrated luminosities used here are 50 fb^{-1} (at 500 GeV), 100 fb^{-1} (at 800 GeV) and 200 fb^{-1} (at 1.0 and 1.6 TeV). In (b) and (c), the $\pm 1\sigma$ contours are displayed for ZZZ / WWZ final states at $\sqrt{s} = 0.5$ and 1.6 TeV respectively, with two beam polarizations (90% e^- and 65% e^+); the thick solid lines present the combined bounds at 90% C.L.

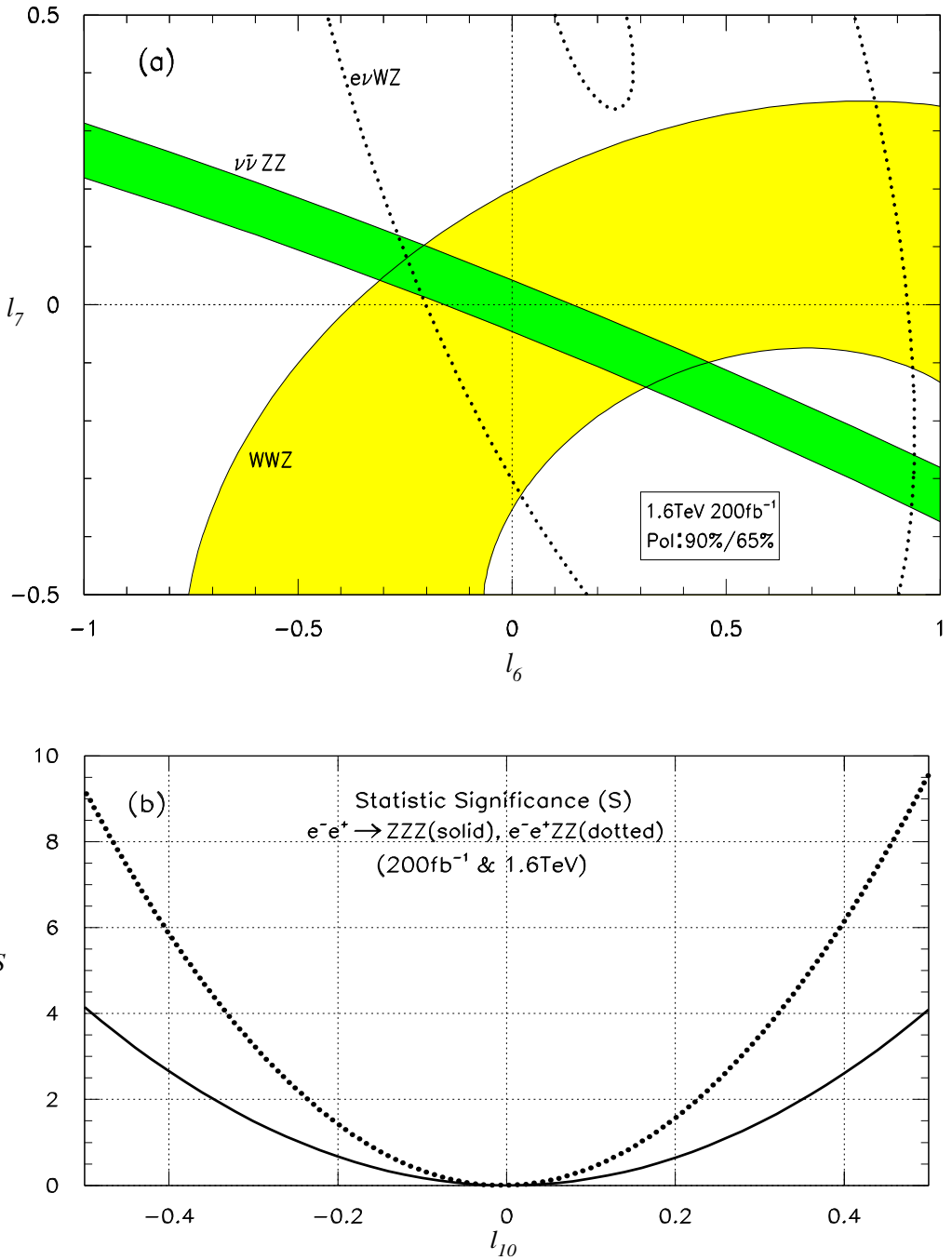


FIGURE 4. Interplay of the WW -fusion and WWZ/ZZZ -production for discriminating the $SU(2)_c$ -breaking parameters ℓ_6 - ℓ_7 and ℓ_{10} at $\sqrt{s} = 1.6$ TeV with $\int \mathcal{L} = 200 \text{ fb}^{-1}$: (a). $\pm 1\sigma$ exclusion contours for $e^- e^+ \rightarrow \nu \bar{\nu} ZZ$, $e^+ \nu W^- Z/e^- \bar{\nu} W^+ Z$, and $e^- e^+ \rightarrow WWZ$ with polarizations (90% e^- and 65% e^+). (b). Statistic significance versus ℓ_{10} for $e^- e^+ \rightarrow ZZZ$, $e^- e^+ \rightarrow ZZ$ (with unpolarized e^\mp beams).